Molecular Therapy
Methods & Clinical Development
Original Article

Differential T cell immune responses to deamidated adeno-associated virus vector

So Jin Bing,[1] Sune Justesen,[2] Wells W. Wu,[3] Abdul Mohin Sajib,[1] Stephanee Warrington,[1] Alan Baer,[1] Stephan Thorgrimsen,[2] Rong-Fong Shen,[3] and Ronit Mazor[1]

[1]Division of Cellular and Gene Therapies, Center for Biologics Evaluation and Research, US Food and Drug Administration, Silver Spring, MD 20993, USA; [2]Immunitrack ApS, Copenhagen, Denmark; [3]Facility for Biotechnology Resources, Center for Biologics Evaluation and Research, US Food and Drug Administration, Silver Spring, MD 20993, USA

Despite the high safety profile demonstrated in clinical trials, the immunogenicity of adeno-associated virus (AAV)-mediated gene therapy remains a major hurdle. Specifically, T-cell-mediated immune responses to AAV vectors are related to loss of efficacy and potential liver toxicities. As post-translational modifications in T cell epitopes have the potential to affect immune reactions, the cellular immune responses to peptides derived from spontaneously deamidated AAV were investigated. Here, we report that highly deamidated sites in AAV9 contain CD4 T cell epitopes with a Th1 cytokine pattern in multiple human donors with diverse human leukocyte antigen (HLA) backgrounds. Furthermore, some peripheral blood mononuclear cell (PBMC) samples demonstrated differential T cell activation to deamidated or non-deamidated epitopes. Also, *in vitro* and *in silico* HLA binding assays showed differential binding to the deamidated or non-deamidated peptides in some HLA alleles. This study provides critical attributes to vector-immune-mediated responses, as AAV deamidation can impact the immunogenicity, safety, and efficacy of AAV-mediated gene therapy in some patients.

INTRODUCTION

Human gene therapy (GT) using viral vectors has shown great promise as a treatment avenue for rare and monogenic disorders that lack alternative treatment options. In GT, recombinant adeno-associated viral (rAAV) vectors are among the most commonly used vectors due to their ability to transduce a wide range of dividing and non-dividing cells, diverse tissue tropism, and episomal expression. Natural infection with AAV is nonpathogenic, but exposure to rAAV vectors in large quantities by unnatural routes can present safety issues. Currently, rAAV accounts for 24% of the viral vectors used in clinical trials worldwide,[1] with more than 100 investigational new drug (IND) submissions for rAAV-based products in the past few years.[2] Furthermore, a number of rAAV gene therapy programs have matured to advanced clinical development[2] or have been approved for licensure.[3,4]

While the number of rAAV-vector-based clinical investigations has been rapidly increasing, significant challenges remain due to the inherent immunogenicity of the rAAV capsid, which largely dictates the interaction of the rAAV with the host immune system. To this end, several studies have shown that engagement of both the innate and adaptive arms of the immune system[5,6] with rAAV impacts the safety and efficacy of the gene therapy.[7] This, in part, is due to widespread exposure of humans to naturally occurring AAV, resulting in pre-existing immunity in 30%–60% of the human population, which typically varies by age and country of residency.[8–10] While humoral immune responses to AAV could be controlled or predicted by measuring pre-existing AAV antibody titers in the serum before or during clinical trials, cellular immune responses to rAAV have been challenging. Deleterious capsid cytotoxic T lymphocyte (CTL) responses have been involved in loss of efficacy and potentially liver toxicities. A loss of factor IX transgene expression and transient mild elevations of liver enzymes in circulation were correlated with $CD8^+$ T cell responses against the rAAV capsid in the first liver-directed gene therapy trial with rAAV.[7,11] It was later shown that transduced cells present capsid-derived epitopes to cytotoxic $CD8^+$ T cells via major histocompatibility complex class I (MHC class I).[12] Recent clinical trials using rAAV also indicated that high abundance of CpG motifs in the vector resulted in failure to achieve sustained expression, owing to capsid-specific $CD8^+$ T cells.[13]

MHC class I and class II molecules have evolved to bind short peptides and present them to circulating T cells and trigger an immune response.[14] The recognition of these peptides by T cell receptors (TCRs) can be highly specific to a point where any minor change in the peptide-MHC complex interaction can drastically affect T cell activation. Post-translationally modified epitopes can alter the molecular fingerprint of the interacting surfaces in TCR/peptide/MHC complexes, potentially affecting immune reactions in an unanticipated manner.[15,16]

Specifically, asparagine deamidation, which is the most common spontaneous post-translational modification,[17] can result in an irreversible

Received 3 November 2021; accepted 16 January 2022;
https://doi.org/10.1016/j.omtm.2022.01.005.

Correspondence: Ronit Mazor, Division of Cellular and Gene Therapies, Center for Biologics Evaluation and Research, US Food and Drug Administration, 10903 New Hampshire Avenue, Building 52/72, Room 3124, Silver Spring, MD 20993, USA.
E-mail: ronit.mazor@fda.hhs.gov

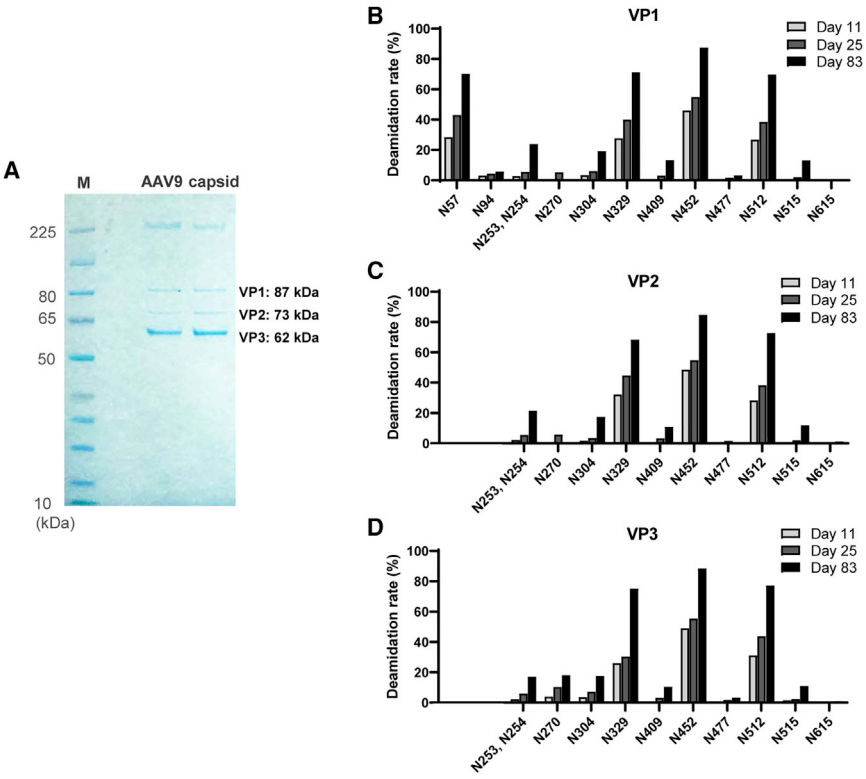

Figure 1. Deamidation occurs in NG site of VP1, VP2, and VP3 AAV9 proteins

At 11, 25, and 83 days after production of AAV9 protein, VP1, VP2, and VP3 were separated by SDS-PAGE and analyzed for deamidation. (A) SDS-PAGE gel showing the viral proteins present in the AAV9 vector. VP1, VP2, and VP3 were separated by denaturing and SDS-PAGE electrophoresis followed by Coomassie blue staining. Three major bands that correspond to VP1 (87 kDa), VP2 (73 kDa), and VP3 (62 kDa) were cut and used for mass spectrometry analysis. M, Spectra Multicolor Broad Range Protein Ladder gel. Expected ratio is VP1:VP2:VP3 = 1:1:10. (B–D) Eluted VP1 (B), VP2 (C), and VP3 (D) proteins from SDS-PAGE were analyzed by LC-MS. Deamidation fractions were calculated based on the number of peptides with D or iD out of the total of the N, D, and iD peptides.

sequence change from asparagine (N) to aspartic acid (D) or to isoaspartic acid (iD). Such changes in amino acid sequences may alter MHC binding or TCR recognition and thus have a significant impact on immune recognition.[18,19] It has been reported that deamidation of six asparagine sites in an anthrax toxin vaccine significantly diminished vaccine efficacy.[20] A converse impact has been demonstrated in a murine autoimmune model of cytochrome *c* (Cyt C), where modifications of "D" amino acid to "iD" amino acid induced a dramatic T cell response and resulted in epitope spreading and an autoimmune response that was cross-reactive to the native Cyt C protein. Furthermore, it has been suggested that deamidation could influence antigen processing and presentation[21,22] or trigger strong auto-reactive B and T cell responses.[23]

Recent studies have demonstrated that recombinant AAV capsids undergo high levels of deamidation.[24,25] Giles et al.[24] found that the highest levels of deamidation in rAAV occur at asparagine residues where the N+1 residue is glycine (i.e., NG pairs) and that deamidation of the rAAV is comprehensive and is not serotype specific or impacted by the manufacturing system. Furthermore, they showed that deamidation also affects capsid assembly, which altered the *in vitro* transduction efficiency in human-liver-derived Huh7 cells.[24] Considering that reported T cell epitopes in rAAV contain NG pairs,[26,27] it is important to elucidate whether naturally occurring deamidation has any impact on the immunogenicity of rAAV.

In this study, we explored the immunological consequences of rAAV deamidation. HLA bindings and T cell reactivity to AAV9-derived peptides that were deamidated or non-deamidated (wild type [WT]) was compared using HLA molecules and human peripheral blood mononuclear cells (PBMCs). Among multiple donors, two of the four NG sites in AAV9 contain CD4 T cell epitopes with a Th1 cytokine pattern. Some PBMC samples had differential T cell activation to deamidated or WT epitopes. This differential response was also observed in peptides derived from other AAV serotypes and was highly impacted by the HLA makeup of the individual. HLA binding assays confirmed the preferential binding of the deamidated or WT peptides to some HLA molecules, including HLA class II DRB1*03:01 and DRB3*02:02. These results indicate that naturally occurring deamidation can significantly affect the immunogenicity of rAAV gene-therapy products.

RESULTS

AAV9 viral capsid proteins VP1, VP2, and VP3 have four major deamidation sites

AAV capsid is primarily composed of three distinct viral proteins, VP1, VP2, and VP3. In order to identify deamidation sites in the AAV9 capsid and compare the magnitude of deamidation among the capsid subunits as well as among lots stored for different lengths of time, three lots of purified rAAV9 were produced. Intact viral capsid was denatured and separated by gel electrophoresis 11, 25, and 83 days after purification (Figure 1A). Gel bands were excised and subjected to in-gel tryptic digestion. Tryptic peptides were extracted from the gels, filtered, and analyzed for deamidation by liquid chromatography-mass spectrometry (LC-MS). Figure 1B shows a total of four distinct major deamidation sites within VP1, with more than 30% deamidation observed in AAV9 capsids that were produced 25 days prior. This deamidation rate was decreased in rAAV produced 11 days prior and was increased an additional

2-fold in rAAV produced 83 days prior. These four sites also coincide with NG sites in AAV9 VP2 and VP3 proteins. No other major differences in these deamidation sites were observed in the common amino acids among VP1, VP2, and VP3. Of note, N57 and N94 are only present in VP1, which has a longer sequence than VP2 and VP3. These data suggest that there is a correlation between the level of deamidation and the time elapsed since the production of the AAV product.

In silico HLA binding analysis predicts potentially promiscuous binders at VP deamidation site

To investigate whether these deamidation sites are located within or near the promiscuous binders in AAV9 capsids that indicate potential T cell epitopes, we carried out predictive modeling of class I and class II MHC-restricted potential epitopes for AAV9 VP1 capsid protein using the Immune Epitope Database (IEDB). To start, 27 HLA class I and 27 HLA class II alleles, representing the most common specificities in the human population and commonly shared binding specificities (i.e., supertypes),[28,29] were submitted for binding prediction to the IEDB, and the percentile rank of each peptide to each allele was recorded. A peptide was considered as an immunodominant promiscuous binder if more than six alleles showed the upper first percentile of binding strength in HLA class I and five alleles showed the upper 10th percentile of binding strength in HLA class II predictions (Figures 2A and 2C, red). This analysis respectively identified 14 and 9 class I and class II potential binders. The majority of the binders were predicted in the VP3 region of AAV9 that is common to VP1, VP2, and VP3,[30] with only two class-I-predicted binders and no class-II-predicted binders in the VP1 unique sequence.

Next, we examined whether any of the deamidation sites coincided with the predicted promiscuous binders. Two deamidation sites in N329 and N452 coincide with predicted HLA class II binders, which were ranked 9 and 2 based on promiscuity rank. None coincident with class-I-predicted binders were observed (Figures 2A and 2C, yellow).

HLA binding for WT or deamidated peptides identifies differential binding affinity

Next, we focused on investigating the binding affinity of deamidated peptides using IEDB prediction and an HLA/peptide stability assay. The prediction score for a peptide-allele pair is given in terms of the percentile rank of the predicted binding strength of 9-mer or 15-mer peptides with or without deamidation. Thus, there were 9 or 15 possible deamidated peptides in which asparagine was converted to aspartic acid. Examples of variant sequences are shown in Figure S1. Figures 2B and 2D show the minimum percentile rank among the 9 or 15 possible deamidated peptides for each allele. HLA class II binding prediction showed promiscuous and differential predicted binding to WT and deamidated peptides. Major class II binding was observed in peptides surrounding N329 and N452 and their deamidated forms. Both were predicted to be most promiscuous for HLA-DRB alleles, with 12 and 11 alleles of the 27 predicted alleles to bind <10% to N452 and N452D, respectively. Interestingly, N512 was predicted to bind with <10% to only two alleles, while the deamidated form N512D was predicted to bind with <10% to six alleles (Figure 2D). Four alleles (HLA-DRB1*03:01, HLA-DRB3*01:01, HLA-DQA1*01:01/DQB1*05:01, and HLA-DQA1*05:01/DQB1*02:01) had a striking decrease in percentile rank, which indicates increased binding to N512D compared with N512 from 26%, 39%, 13%, and 19%–3.8%, 3.5%, 3.9%, and 9.7%, respectively. One allele, HLA-DRB3*02:02, showed a converse trend with higher binding to WT N512 (1.5%) predicted than to deamidated peptide (5%).

HLA class I did not have as much breadth of binding (no peptide had greater than six alleles predicted to bind <1%) as HLA class II (Figure 1B). However, differential binding that may result in high-affinity presentation of WT or deamidated peptides was observed in HLA-A*01:01, HLA-A*02:01, and HLA-B*44:02, where deamidation increased the binding between the HLA and the peptide, and HLA-A*02:03, HLA-A*30:01, HLA-A*30:02, HLA-A*32:01, HLA-B*08:01, and HLA-B*15:01, where deamidation caused a decrease in binding.

To confirm the binding affinity experimentally and examine the impact of isoaspartic acid on the binding, four sets of 9-mer and four sets of 20-mer peptides were synthesized. Each set includes a WT and two deamidated peptides (aspartic acid or isoaspartic acid forms). The sequences and purity of peptides are shown in Table S1. The binding affinities of 9-mer peptides to 12 HLA class I and 20-mer peptides to 12 HLA class II were assessed by comparing the peptide-MHC complex stability to that of positive control peptides. Figures 3A and 3B show that some HLA class I presentation molecules, such as HLA-A*02:03 and HLA-B*15:01, and class II molecules, such as HLA-DRB1*01:01 and HLA-DRB5*01:01, bind with higher stability to WT peptides. On the other hand, other HLA class I presentation molecules, such as HLA-A*02:01, HLA-B*44:02, and HLA-B*44:03, and class II presentation molecules, such as HLA-DRB1*03:01 and HLA-DRB3*02:02, show preferred binding to the deamidated N512 peptides. Most parts of these data were correlated with our *in silico* prediction. For example, HLA-A*02:03 had very strong binding to WT peptides N452 and N512 but weak binding to the deamidated peptides. Conversely, HLA-DRB1*03:01 had no binding to the WT N512 peptide but had very strong binding to the deamidated peptide. Of note, no major binding was observed between any HLA and peptides that contained isoaspartic acid when compared with the blank control ($p > 0.05$). These *in silico* predictions and experimental binding data implicate that deamidation could increase or decrease T cell activation.

Deamidation of AAV9 peptides affect cytokine production

To confirm whether the deamidation altered the host immune response, PBMCs from 30 healthy donors were incubated with peptide pools for 10 days, followed by restimulation with single peptides. Details of the peptide pools are given in Table S1, and HLA alleles are shown in Tables S2 and S3. Responses were measured by interleukin-2 (IL-2) and interferon gamma (IFN-γ) enzyme-linked immunosorbent spot (ELISpot) assay. Heatmaps demonstrating the T cell responses of the 30 donors are shown in Figures 4A and 4B. Among the 30 donors, 7 donors did not show any positive responses by either

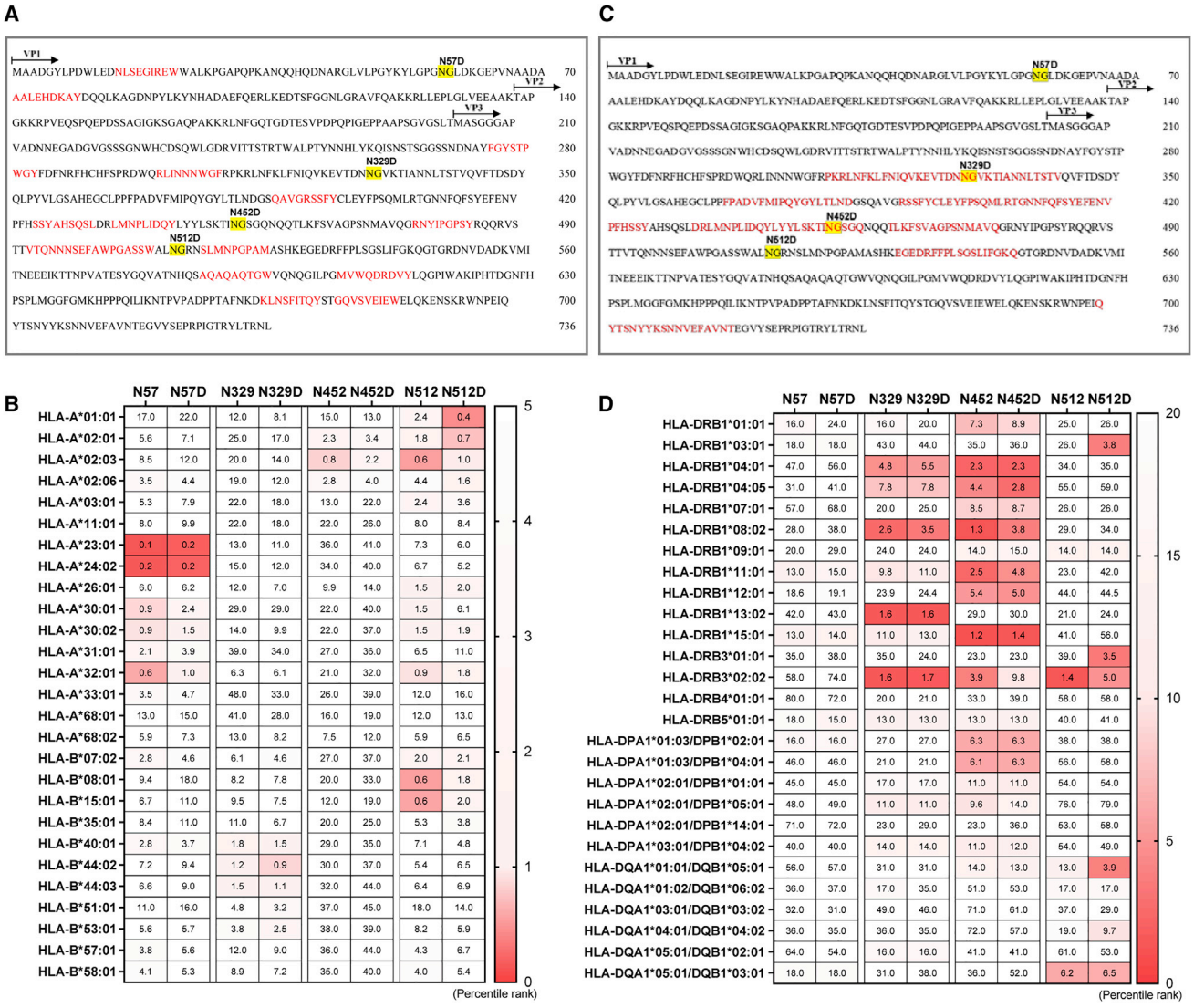

Figure 2. Deamidation sites within the MHC class I and MHC class II predicted binders of AAV9 capsid

Predicted binding of WT or deamidated sequence-modified peptides to MHC class I (A and B) or MHC class II (C and D) reference set. (A and B) Predictions were generated using the "recommended IEDB 2020.04," which defaults to the NetMHDpan EL4.0 method. (C and D) Predictions were generated using the "recommended IEDB method," which defaults to the IEDB consensus method when combined consensus scores are possible. (A and C) Sequence of the AAV9 capsid protein VP1 region with the predicted class I or II HLA epitope regions (red font, A; count if <1 is over 6/27, C; count if <10 is over 5/27 and deamination sites [highlighted in yellow] are shown). (B and D) The percentile ranks predicted by the IEDB method for recommended 27 HLA class I (B) and class II (D) alleles. The upper 1st (B) or 10th (D) percentiles of binding strength were considered the strongest binders and are colored in red.

IL-2 or IFN-γ production. There were strong immune responses to WT or deamidated peptides by producing IL-2 and IFN-γ more than 3-fold above background in 14 donors. No significant responses with any of the 9-mer peptides in the IL-2 and IFN-γ ELISpot were observed (data not shown). Restimulation with the 20-mer peptides not only gave responses but showed differential IL-2 and IFN-γ activation between WT and deamidated forms. IL-2 response rates to WT peptides in N57, N329, N452, and N512 regions were 37%, 47%, 40%, and 17%, respectively (Figure 4C). The rates of responses were reduced when cells were restimulated with deamidated peptides. The IFN-γ responses were relatively less detectable (Figure 4D), possibly due to higher nonspecific background levels (Figure S2), but the response trend was similar to IL-2 responses (Figures 4D and 4F). In a total of 14 donors, T cell responses to the peptide within the N329 region were generally weaker in the deamidated form (Figure 4E). Deamidation at the N452 site resulted in an induction of T cell responses in nine donors in comparison with a decrease in T cell responses in another nine donors (Figure 4E). As shown in Figure S2, in comparison with the WT-peptide-treated group, deamidated peptide at the N452 region showed substantially lower IL-2

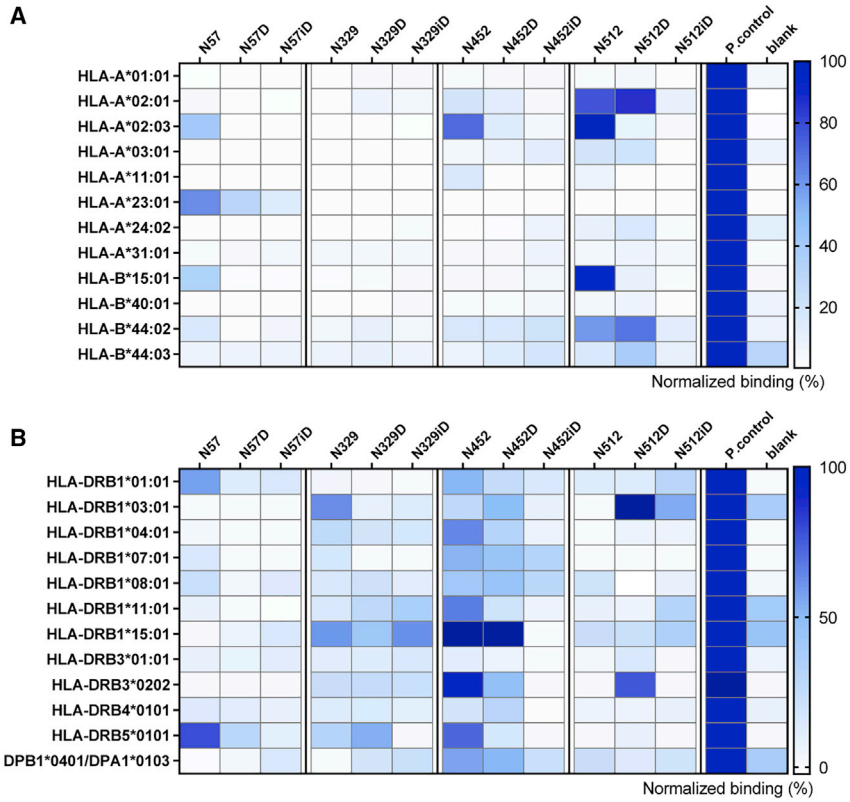

Figure 3. Differential HLA binding to WT and deamidated peptides

Stabilities of peptide binding to HLA class I (A) or HLA class II (B) were assessed by MHC/peptide stability assays using denatured and biotinylated HLA molecules (Immunitrack Aps). Measurements were performed in duplicate and normalized to the positive control.

and IFN-γ responses in donor no. 4, whereas the same peptide resulted in significantly higher responses in donor no. 6 in comparison with WT-peptide-treated group. The response rates to peptides in the N57 region were unexpectedly higher than expected based on *in silico* and binding affinity data. The peptides with the N512 region did not stimulate cells from many donors, but four donors (nos. 17, 29, 36, and 55) showed higher responses to the deamidated form of the peptide, while three donors (nos. 4, 7, and 57) responded more to the WT form. Interestingly, 75% of the donors (nos. 29, 36, and 55) that showed higher responses with deamidated peptides carried HLA-DRB1*03:01, whereas none of the responders with WT peptide were HLA-DRB1*03:01 carriers, suggesting that the deamidated form of peptide may be preferably recognized by HLA-DRB1*03:01 alleles in agreement with Figures 2 and 3.

Additional examination of tumor necrosis factor alpha (TNF-α) response did not show any clear differences, presumably due to high background levels as evidenced in our media only control group (Figure S2). These data indicate that the spontaneously occurring deamidation in AAV alters the T cell responses to produce IL-2 or IFN-γ, and it is highly donor specific.

CD4 T cells are the main responders to AAV peptide stimulation

Based on the observations that (1) peptides at the deamidation sites are predicted by the IEDB prediction tool to strongly bind HLA class II (Figure 2), (2) increased binding to HLA class II was observed in the MHC/peptide stability assay (Figure 3), and (3) IL-2 responses against peptide stimulation were readily detectable in the ELISpot assay (Figure 4), it was hypothesized that cell responses against peptides at the deamidation sites are CD4 T cell mediated. To phenotype the cellular subsets involved in the immune response to the peptides at the deamidation site, expanded PBMCs were restimulated with the four WT peptides for 24 h, followed by flow cytometry analysis. Measured IL-2, IFN-γ, and TNF-α secretion in CD4 T cell, CD8 T cell, γδ T cell, and natural killer (NK) cell subsets is shown in Figure S3. Figures 5A–5D show a representative response of one donor after restimulation with peptide N452. In agreement with the ELISpot results, we found that peptide N452 triggered cells to produce cytokines (Figure 5A). To identify the cells that were responding to peptide stimulation and producing cytokines, the absolute number of each subset after gating on the cytokine-secreting cells was analyzed. Figures 5B–5D demonstrate that the number of cytokine-producing CD4 T cells was significantly increased by peptide stimulation. Similar CD4-mediated responses against peptide stimulation by other peptides with several additional donors were further confirmed (Figure S4). In addition, multiparametric analysis permitted the precise characterization of this CD4 T cell subset as that of $CCR7^{-}CD45RA^{-}$ effector memory (EM) cells (Figures 5E–5G).[31] This suggests that T cells that were activated are almost exclusively CD4 EM cells.

Deamidation of AAV9 peptides affects cytokine production from CD4 T cells

Since flow cytometry analysis pointed to the activation of CD4 T cells in response to the peptides at deamidation sites, further evaluation was done to determine whether the deamidation alters the CD4 cell response. PBMCs were thus restimulated with WT or deamidated peptides for 24 h and analyzed using flow cytometry. The gating strategy is shown in Figure S3. IL-2-, IFN-γ-, TNF-α-, and IL-4-positive cells in the $CD4^{+}$ gate from peptide stimulation were normalized to a media control group. Figure 6 shows the fold changes of cytokine-producing CD4 cells in peptide-treated groups compared with a media control. Similar to the findings in ELISpot assay (Figure 4), cytokine production from CD4 T cells was stronger with WT peptides in some donors, whereas deamidated peptides showed higher responses in other donors.

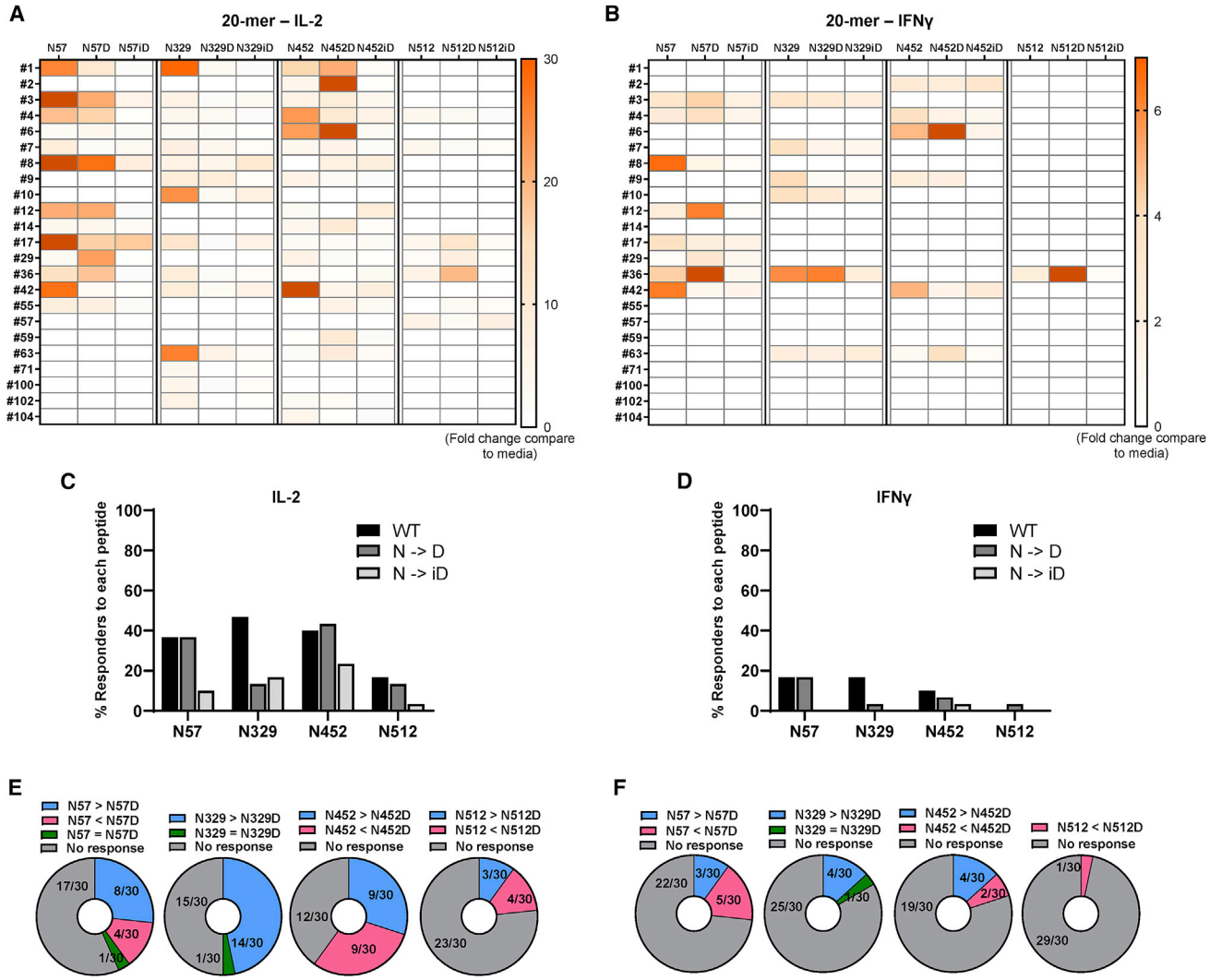

Figure 4. Differential PBMC responses to WT and deamidated peptides

Cells from healthy donors were stimulated with either WT or deamidated peptides and expanded for 10 days. Cells were restimulated with individual WT or deamidated peptides. (A and B) After 24 h, IL-2- (A) and IFN-γ (B)-producing cells were detected by ELISpot assay. Number of spots for IL-2 and number × size of spots for IFN-γ were analyzed. Each value indicates fold change relative to their respective media-only control (stimulation index). (C and D) Percent of PBMC samples that show IL-2 (C) or IFN-γ (D) responses (stimulation index >3) to all 20-mer peptides. (E and F) Differences in IL-2 (E) or IFN-γ (F) secretion between WT and deamidated-peptide-treated PBMCs. Blue color indicates lower IL-2 production after restimulation with deamidated peptides (the ratio of deamidated group to the WT group is below 0.9). Pink color indicates higher IL-2 production after restimulation with deamidated peptides (the ratio of deamidated group to the WT group is above 1.1). Green color indicates no change in IL-2 production between the WT and the deamidated-peptide-treated group (the ratio of deamidated group to the WT group is between 0.9 and 1.1).

However, IL-4 secretion in $CD4^+$ T cells did not show significant differences between WT and deamidated-peptide-stimulated groups. Representative flow cytometry plots are shown in Figure S5. Figures S5A and S5B show a strong CD4 T cell activation in response to WT peptide and a weak or no response to the deamidated peptides. Conversely, Figures S5C and S5D show a significant increase in CD4 cytokine production after stimulation with deamidated peptides.

There were no significant changes in cytokine production by CD8 T cells between WT and deamidated peptide groups (Figure S6). Differential CD4 T cell responses of WT and deamidated-peptide-stimulated groups were confirmed by an independent ELISpot assay using isolated CD4 T cells by negative magnetic-activated cell sorting (MACS) selection (Figure S7). Together, these results suggest that deamidation sites contain CD4 T cell epitopes.

Differential immune responses caused by deamidation are not serotype specific

To investigate whether the differential immunogenicity of deamidated AAV9 also occurs in other AAV serotypes, we first compared

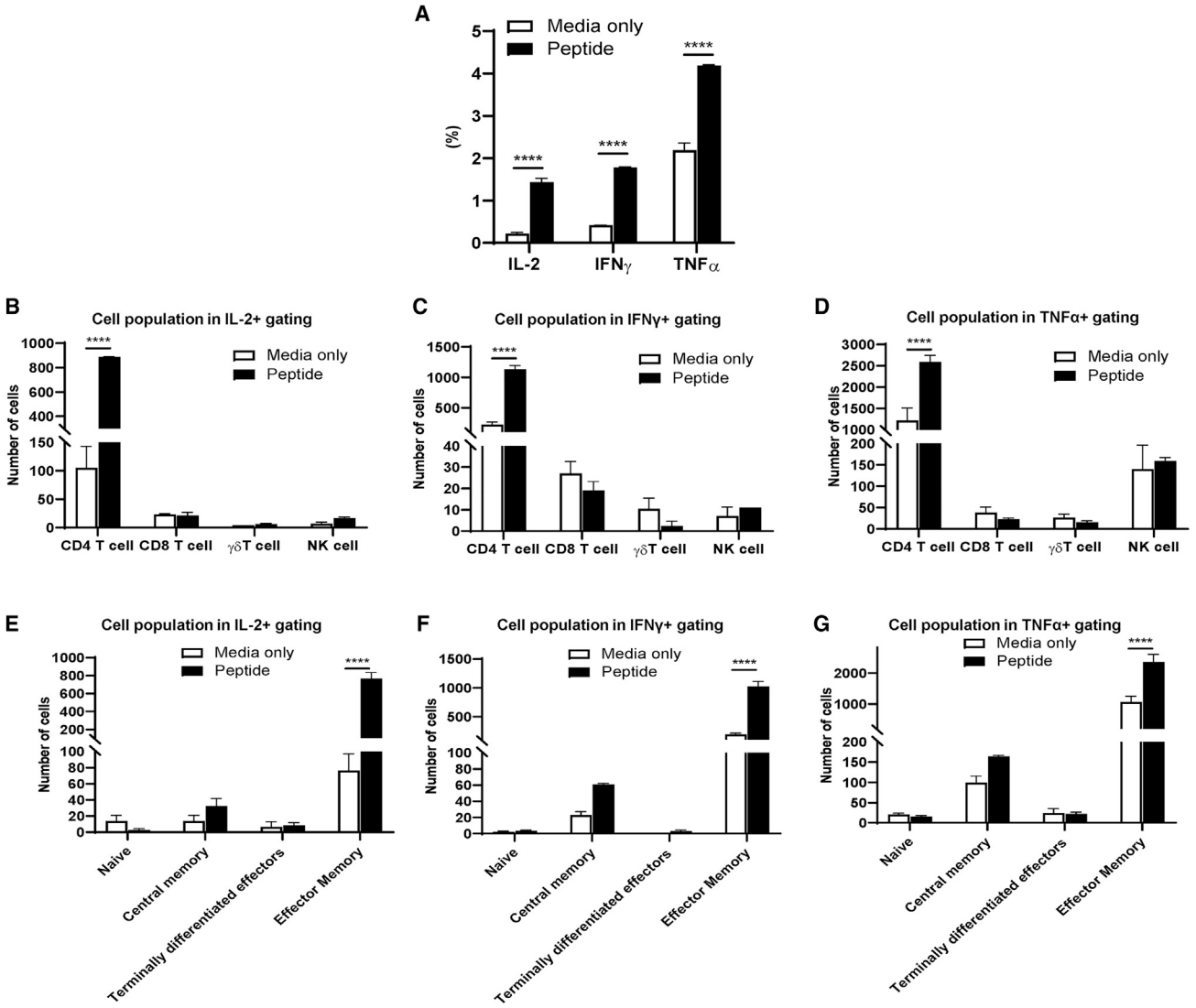

Figure 5. AAV-derived peptides stimulate effector memory CD4 T cells to produce cytokines

Cells from a representative donor (no. 42) were expanded with peptide pools for 10 days and restimulated with N452 peptide (20-mer) for 1 day. (A) IL-2-, IFN-γ-, and TNF-α-producing cells in lymphocytes were analyzed. (B–D) Within the IL-2- (B), IFN-γ- (C), or TNF-α (D)-positive cells, the number of CD4 ($CD4^+CD8^-CD3^+TCR\gamma\delta^-$), CD8 ($CD4^-CD8^+CD3^+TCR\gamma\delta^-$), γδ T (TCR $\gamma\delta^+CD3^+$), and NK ($CD56^+CD3^-$) cells were counted. (E–G) Within the IL-2- (E), IFN-γ- (F), or TNF-α (G)-positive CD4 T cells, the number of naive ($CCR7^+CD45RA^+$), central memory ($CCR7^+CD45RA^-$), terminally differentiated effector ($CCR7^-CD45RA^+$), and effector memory ($CCR7^-CD45RA^-$) cells were counted. Each bar shows the mean ± SD. ****$p < 0.0001$. p values were determined by ANOVA with Tukey's multiple comparisons test.

the amino acid sequences of AAV1–AAV13. Results showed seven more NG sites in other AAV serotypes (Table S4). We further investigated whether the deamidation of other NG sites impacts the immune response against AAV. Binding affinities of peptides at seven NG sites derived from other serotypes for 27 recommended HLA class I or class II alleles were predicted using the IEDB analysis tool. Peptides with N264, N383, N540, N546, and N718 regions were predicted to be strong binders (the upper first percentile), with at least four different HLA class I alleles (Figure S8). In addition, peptides in the N383 and N540 regions were predicted to strongly bind with HLA class II alleles (Figure S9). Peptides were then synthesized with either WT or deamidated forms (Table S5), and HLA binding stability of the peptides to 12 HLA class I and 12 HLA class II was assessed. Figure S10 displays that some WT peptides strongly bind to HLA-A*02:01, HLA-A*02:03, HLA-A*23:01, HLA-A*24:02, HLA-B*15:01, HLA-DRB3*01:01, and HLA-DRB3*02:02, while some deamidated peptides preferentially bind to HLA-B*44:02. Specific T cell responses to particular peptides were measured using IL-2 and IFN-γ secretion ELISpot assays with PBMCs from four healthy individuals. The immune responses against peptides at the deamidation sites in other AAV serotypes were similar to those of AAV9. N718 peptide, derived from AAV1 and AAV6, had a decreased IL-2 response after

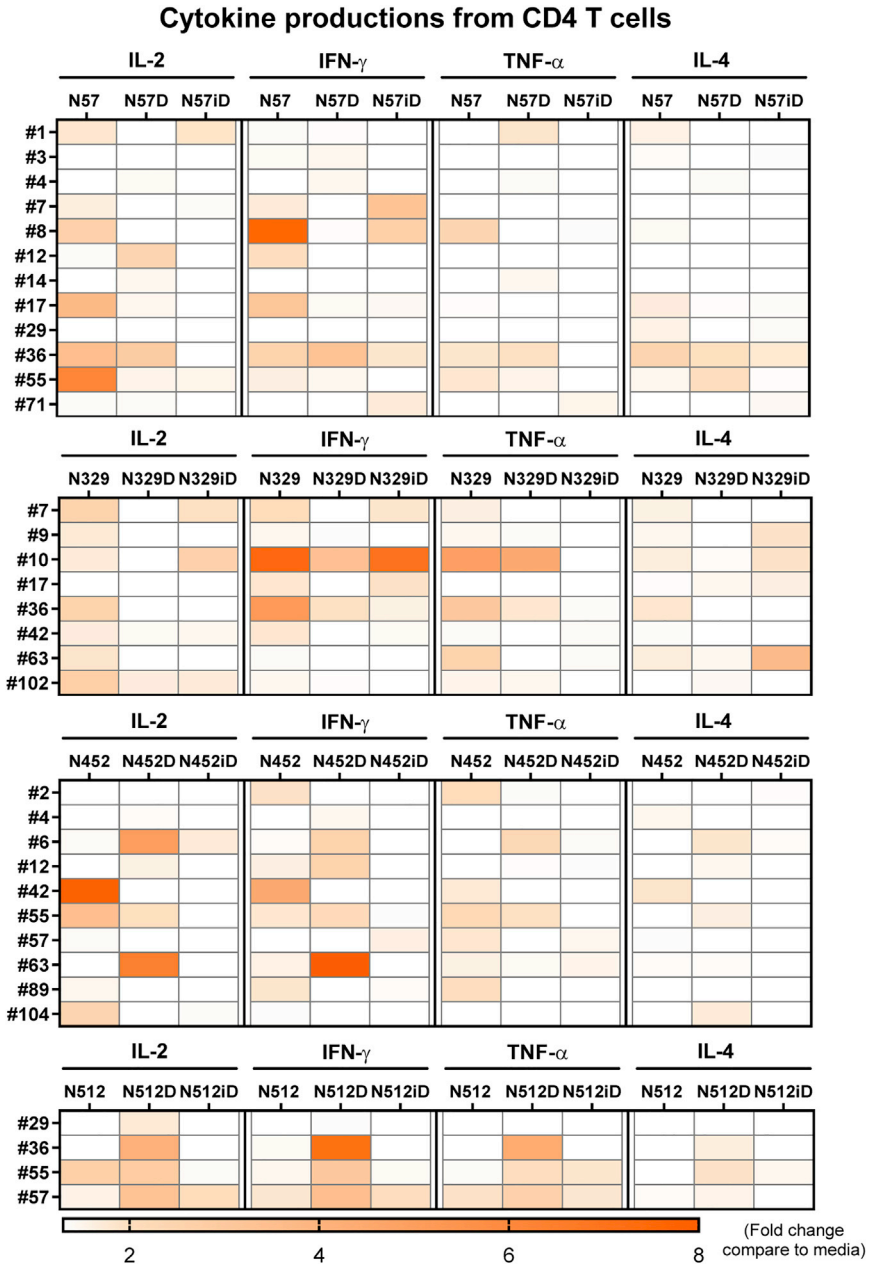

Figure 6. Differential cytokine production from CD4 T cells after stimulation with WT or deamidated peptides

Cells from healthy donors were stimulated with either WT or deamidated peptides and expanded for 10 days. Flow cytometric analysis shows IL-2, IFN-γ, TNF-α, and IL-4 staining of $CD4^+$ T cells, 24 h after restimulation of PBMCs with individual WT or deamidated peptides. Each value indicates fold change relative to their respective media-only control.

stimulation with WT N718 peptide, but not with deamidated N718D peptide. Whereas 20-mer peptides at the N540 region derived from AAV8 displayed enhancement of IL-2 secretion, stimulation with deamidated peptides resulted in much lower secretion (Figure S11). These data suggest that differential immune responses caused by deamidation are not serotype specific.

DISCUSSION

The immune response to rAAV gene therapy remains a major limiting factor in its successful implementation and is closely correlated to treatment outcomes, particularly in regard to transgene expression longevity and the ability to re-administer the vector. Prior studies have shown that rAAV vectors undergo a high degree of spontaneous deamidation, with the highest levels occurring at NG pairs on the AAV vector capsid, and that this functionally impacts transduction efficiency.[24] In the present study, we further characterized the deamidation to the VP subunits and the duration of rAAV storage and performed *in silico* prediction and various immunological assays to study the effects of deamidation on the immunogenicity of rAAV. Deamidation in rAAV resulted in either reductions or enhancements in the immunogenicity of rAAV. These results were highly donor specific and dependent on particular deamidation sites in rAAV. Furthermore, CD4 Th1 effector memory cells play a major role in this immune response, demonstrating the pivotal role of CD4 T cell epitopes in the immune response against rAAV.

We evaluated three layers of the T cell immune response to WT and deamidated peptides. We started with an HLA binding prediction that narrowed the list of potential peptides and showed that two HLA class II promiscuous binders coincide with deamidation sites. We further showed that some HLA molecules are predicted to bind with higher or lower affinity to deamidated peptides than WT peptides. To confirm these predictions, we synthesized sets of peptides that had the highest probability of binding to HLA molecules. Each deamidation site was represented by a set of 9-mers and a set of 20-mers and included a WT, a deamidation to aspartic acid, and a deamidation to isoaspartic acid peptide. To validate the binding predictions, 24 HLA molecules were made and tested for their binding to the various peptides. Some correlations between the predicted binders and the experimental binders were observed, confirming that some HLA molecules bind to WT and deamidated (aspartic acid) peptides differentially.

Finally, the T cell immune response was evaluated using expanded PBMCs from untreated donors. Most of the samples responded to both WT and deamidated peptides. Importantly, one deamidated site (N512) had a tendency to induce T cell activation in some samples that share HLA-DRB1*03:01. The immune response to the deamidated peptides was characterized as $CD4^+$ EM with a Th1 cytokine signature. This indicates that the spontaneously occurring deamidation in AAV may increase the immunogenicity of AAV in some individuals. Furthermore, due to the high level of deamidation in AAV, it may be informative to include these deamidated peptides in cellular immune monitoring during clinical trials.

Although there are two prior studies that mapped T cell epitopes in AAV2,[26,27] CD4 T cell epitopes have not been identified, despite their critical roles in generating the complex humoral and cellular immune responses to AAV.[32] In this study, we identified CD4 T cell epitopes on the AAV9 capsid that coincide with two deamidation sites. Consistent with the previous reports that characterized the immune response to AAV1 and AAV2,[33,34] we found that the AAV9-specific CD4 T cells produced Th1-type cytokines and belonged mainly to the effector memory subset. This observation may have implications for vector re-administration in a pre-clinical or clinical setting, considering the vigorous and efficient responses of memory cells.

HLA binding algorithms can support high-throughput and rapid predictions for hundreds of peptide candidates. The accuracy of such prediction methods is improving rapidly, and their use is becoming more acceptable.[35–37] However, they are still hindered by the risk of false-positive and false-negative predictions.[38,39] To validate the binding predictions, we performed *in vitro* HLA binding assays in 12 HLA class I alleles and 12 class II alleles. The choice of alleles was determined by binding core coverage and MHC molecule availability.[28,29] Indeed, the HLA binding assays corroborated several of the *in silico* predictions. For example, peptide N452 was predicted to bind with high affinity to most HLA class II DR alleles, but not to most HLA class I. More specifically, only HLA class I A*02:03 was predicted to bind with ranking of <1%. *In vitro* HLA binding showed a very similar result in that 9/12 of HLA class II DR alleles had >40% binding to class II but only a single HLA class I allele.

While HLA binding assays can detect possible binding of a peptide to the MHC grove, T cell activation assays require the critical steps of MHC-peptide complex presentation to T cells and T cell activation.

A potential concern while working with peptides that contain NG sites is that the peptides could undergo deamidation, which could impact the integrity of our results. To eliminate this concern, peptide sequence and purity were confirmed twice using LC-MS, before and after the peptides had been resuspended and frozen. Peptide integrity was conserved throughout the study. Peptides were further tested for endotoxin content to assure the immune response was specific to the peptide sequences. This assures that the immunological changes observed in the study were not due to nonspecific contaminates and that WT peptides did not undergo spontaneous deamidation.

We observed that most donors who showed stronger T cell responses with deamidated peptide (N512D) were carrying HLA-DRB1*03:01. This shares a similar concept with the known predisposition of individuals with HLA haplotypes DQ2 and DQ8 (HLA-DQB1*02:02 and DQB1*03:02) to develop celiac disease as a response to deamidated Gln in gliadins from dietary wheat gluten. Mapping of the immunodominant T cell epitopes in complex with HLA DQ2 and DQ8 revealed that the deamidated Gln residues induce strong binding of the peptides by acting as high-affinity anchors.[16,40] In addition, very few responses were observed after stimulation with peptides that contained isoaspartic acid. This is consistent with the notion that many non-natural amino acids have diminished binding to MHC molecules.[41,42]

Immune-mediated liver toxicities are a major concern during AAV gene therapy clinical trials.[7,43,44] To monitor AAV-targeting T cells that are associated with these liver toxicities, many investigators use cellular T cell activation assays.[45] These assays often involve PBMCs isolated from patients' blood, followed by restimulation of the cells with overlapping peptides that span the entire AAV VP1 amino acid sequence.[46,47] Our findings, however, suggest that some individuals responded to the deamidated peptides, but not to the WT peptides. The absence of deaminated peptides in these cellular T cell activation assays could result in a potential failure to detect critical and relevant immune response in these individuals.

Deamidation is a chemical process that occurs over time. We note that the observed deamidation rate in the newer AAV batch that was purified and frozen only 11 days prior to the MS analysis was lower than the deamidation rates of the other batches that were prepared 25 and 83 days before analysis. This observation is consistent with other therapeutic proteins like monoclonal antibodies[48] and may be considered a critical quality attribute for rAAV manufacturing. Furthermore, it stands to reason that rAAV storage conditions may benefit from extensive formulation studies with a focus on deamidation prevention.[49]

Our study evidenced the difficulty of predicting the impact of rAAV-capsid-specific cellular immunity on the safety of rAAV-based gene-therapy products, as subtle deamidations may significantly enhance or reduce their immunogenicity. Our results indicate that inclusion of both WT and deamidated peptides in assays used for clinical pre-screening and patient monitoring might be valuable to better understand responses in a small subset of individuals treated with AAV gene therapy.

MATERIALS AND METHODS

Production of AAV9 and quantification

AAV was produced using triple transfection as previously described with some modifications.[50,51] Briefly, free-style 293F cells (Thermo Fisher Scientific, San Jose, CA) were triple transfected with a pscAAV-GFP vector (AAV-410, Cell Biolabs, San Diego, CA), pAAV2/9n (112,865, Addgene, Watertown, MA), and pHelper vector (340,202, Cell Biolabs) in a ratio of 1:1.5:2, respectively. PEI MAX

(Polysciences, Warrington, PA), at a polyethylenimine (PEI):DNA ratio of 2:1, was used as the transfection reagent. At 72 h post-infection, the supernatant was collected and the cell lysate was resuspended in 10 mL lysis buffer and stored at −80°C for 2 weeks. Later, rAAV particles in the supernatant were recovered by polyethylene glycol (PEG) precipitation. The cell lysate was subjected to three freeze-thaw cycles to liberate the virus and treated with 100 U/mL of Benzonase Nuclease (Millipore Sigma, Billerica, MA) for 1 h at 37°C. Cellular debris was removed by centrifugation for 20 min at 10,000 × *g*. Finally, rAAVs were purified using two iodixanol ultracentrifugation gradients and concentrated in 100-kDa concentration columns (Thermo Fisher Scientific). Purified rAAVs were subjected to absolute quantification by Taqman quantitative PCR (qPCR) as previously described.[52] For Taqman qPCR, the following primers and probes were used: EGFP (forward: 5′-AGCAAAGACCCCAACGAGAA-3′, reverse: 5′- GGCGGCGGTCACGAA-3′, and probe: 5′-6FAM-CGCGATCACATGGTCCTGCTGG-TAMRA-3′). The targets were amplified using SsoAdvanced Universal Probes Supermix (1,725,281, Bio-Rad, Hercules, CA), and thermocycling conditions were 3 min at 95°C and then 40 cycles of 95°C for 30 s and 58°C for 30 s on a Bio-Rad iCycler iQ Multicolor Real-Time PCR Detection System.

SDS-PAGE and Coomassie blue staining

SDS-PAGE was performed using 4%–12% Bis-Tris gels (Thermo Fisher Scientific) according to the manufacturer's protocol. Briefly, the gels were loaded with a total volume of 36 μL, which contained 20 μL of AAV9 sample, 10 μL of resuspension buffer, and 10 μL of NuPAGE LDS Sample Buffer (4×) (Thermo Fisher Scientific). Samples were incubated for 10 min at 70°C before loading. Coomassie blue staining was performed by using SimplyBlue SafeStain (Thermo Fisher Scientific) according to the manufacturer's instructions.

In-gel digestion of 1D gel bands

1D gel bands corresponding to VP1, VP2, and VP3 were excised and in-gel digested following the standard protocol at the US Food and Drug Administration's (FDA's) Facility for Biotechnology Resources.[53] Briefly, gel slices were excised, diced into smaller fragments, de-stained with 50% acetonitrile in 25 mM NH_4HCO_3, and then dried. Samples were reduced with 10 mM dithiothreitol in 25 mM NH_4HCO_3 at 56°C for 1 h, followed by alkylation with 55 mM iodoacetamide for 45 min at room temperature. In-gel trypsin digestion was performed using 12.5 ng/μL of sequencing grade modified porcine trypsin (Promega, Madison, WI) diluted in 25 mM NH_4HCO_3 at 37°C overnight. Peptides were extracted from the gel fragments with 5% formic acid and 50% acetonitrile and particulates removed using Ultrafree MC 0.45 μm pore size, hydrophilic polyvinylidene fluoride (PVDF) centrifugal filter (Millipore Sigma). Sample volume was reduced to 5 μL using a speedvac concentrator, reconstituted to final 20 μL of 0.1% formic acid and analyzed by nano-LC/MS/MS.

Mass spectrometry

Trypsin-digested peptides were analyzed by nano-LC/MS/MS using Ultimate LC and Fusion Orbitrap MS (Thermo Fisher Scientific), followed by general settings at the FDA's Facility for Biotechnology Resources.[54] Briefly, peptides were first loaded onto a nanotrap (ThermoFisher PepMap C18, 5 μm, 100Å, 20 mm × 100 μm inner diameter [ID]) and then eluted onto a reversed phase Easy-Spray column (ThermoFisher PepMap C18, 3 μm, 100Å, 15 cm × 75 μm ID) using a linear 120-min gradient of acetonitrile (2%–50%) containing 0.1% formic acid at 250 nL/min flow rate. The eluted peptides were sprayed into the Fusion Orbitrap. The data-dependent acquisition (DDA) mode was enabled. Each Fourier transform (FT) precursor mass MS1 scan (120,000 resolution) was followed by FT MS2 scans (15,000 resolution) using top speed (acquiring as many MS2 scans as possible within 3-s cycle time). Precursor ion fragmentation took place at higher energy collisional dissociation (HCD) cell with collision energy of 30. Automatic gain control (AGC) targets and maximum injection times were set as "standard" and "auto," respectively. The spray voltage and ion transfer tube temperature were set at 1.8 kV and 250°C, respectively.

Nano-LC/MS/MS spectra were processed using Byonic software and further quantitatively analyzed by Byologic software (PMI-Suite 3.8.11, Protein Metrics, Cupertino, CA). Byonic and Byologic search parameters were set according to the parameters employed (tryptic cleavage sites @K/R, 2 mis-cleavage allowed, common modifications of oxidation @M/deamidation @N, fixed modification of carbamidomethylation @C, and PEP 2D/Score/Delta Mod Score being ≤ 0.01, ≥ 100, and ≥ 10, respectively).

In silico HLA binding prediction

Peptide binding affinities for HLA class I and class II alleles were predicted using the MHC I or MHC II binding prediction tool available at the IEDB (www.IEDB.org). MHC class I predictions were generated using the "recommended IEDB 2020.04," which defaults to the NetMHDpan EL4.0 method.[55] MHC class II predictions were generated using the "recommended IEDB method," which defaults to the IEDB consensus method when combined consensus scores are possible.[56] HLA binding ranking was predicted for each 9-mer peptide with 27 HLA class I alleles (Figure 2B)[29] and 15-mer peptide with 27 HLA class II alleles (Figure 2D).[28] These 54 class I and class II HLA alleles represent the most common specificities in the world population and represent commonly shared binding specificities (i.e., supertypes).[28,29] Potential binders in AAV9 VP1 were identified using an initial cutoff of the upper first or 10th percentile of binding strength for HLA class I or class II alleles, respectively, and a promiscuity cutoff of 6/27 or 5/27 alleles.

Peptide synthesis

Examples for 9-mer and 20-mer peptides design are described in Figure S1. The start and end amino acids, as well as the location of the deamidation sites, were determined based on the lowest median predicted percentile rank for the WT peptides (Figure S1). All peptides were synthesized by GenScript Biotech (New Jersey) with the exception of the CEF and CEFT peptide pool controls (PANATecs, Germany). Peptides were purified to >95% homogeneity by high-performance LC (HPLC), and their composition and deamidation were

confirmed twice by MS, once during manufacture release and once after DMSO reconstitution and a freeze thaw cycle. Peptides were dissolved in DMSO at 50 mg/mL and stored at −20°C. For T cell expansion, peptides were pooled into three groups: (1) WT peptides; (2) deamidated peptides with aspartic acid, and (3) deamidated peptides with isoaspartic acid (Table S1).

MHC/peptide binding assay

For MHC I binding assay, urea-denatured and biotinylated MHC samples were diluted into refolding buffer containing nanomolar concentrations of β2m and 2 μM peptides. After 24 h of refolding, the refolded MHC complexes were transferred to a microplate and stressed with 4 M urea. After 3 h, the plates were developed as a conventional ELISA with a conformational specific antibody. In each plate, a reference peptide was used. This peptide is known to bind with high stability to the given allele and was used as a 100% reference. Hence, peptides that gave the same signal in the ELISA as the reference peptide were given a stability of 100%. The MHC II assay was carried out in the same manner. The only difference was that β2m was omitted and both the alpha and biotinylated beta chains were urea denatured and diluted to nanomolar concentrations in refolding buffer containing 2 μM peptide. Final concentrations of b2m, MHC I heavy chain, and MHC II alpha and beta chains were carefully adjusted to ensure the highest possible signal-to-noise ratio between samples with peptide and no peptide. For MHC II, a mixture of hemagglutinin (HA) 306–318, CLIP, and PADRE (YKYVKQNTLKLAT, PVSKMRMATPLLMQ, and AKFVAAWTLKAAA) were used as reference peptides.

Human PBMC samples

PBMCs were collected from apheresis samples of 30 healthy donors under protocols approved by the National Institutes of Health Institutional Review Board (CBER-047). Samples were isolated using gradient-density separation by Ficoll-Hypaque (GE Healthcare, Chicago, Illinois) according to the manufacturer's instructions, and the buffy coat was collected and washed three times with phosphate-buffered saline (PBS) without Ca and Mg. PBMCs were cryopreserved in liquid nitrogen at a concentration of 2.5–5 × 10^7 cells/mL in RPMI media (Thermo Fisher Scientific) supplemented with 10% heat-inactivated human AB serum (Millipore Sigma) and 7.5% DMSO (Thermo Fisher Scientific). HLA typing was performed as described previously by Scisco Genetics (Seattle, Washington)[54]. The HLA distribution of the donors is representative of the United States and European populations.[57]

In vitro expansion of PBMCs

For usage, PBMCs were thawed, washed, counted, and resuspended at a concentration of 2 × 10^6 cells/mL in RPMI media containing 5% heat-inactivated human serum, 1% Glutamax (Thermo Fisher Scientific), 1 mM sodium pyruvate (Thermo Fisher Scientific), 10 mM HEPES (Thermo Fisher Scientific), MEM Non-Essential Amino Acids (Thermo Fisher Scientific), and 1% penicillin/streptomycin (Thermo Fisher Scientific). Cells were cultured with peptide pools at a final concentration of 5 μg/mL. Cells were supplemented with fresh assay medium containing 20 units of IL-2 (Millipore Sigma), 5 μg/mL of IL-7 (BioLegend, San Diego, CA), and 25 μg/mL of IL-15 (BioLegend) every 3 or 4 days.

ELISpot assay

The secretion of IL-2 and IFN-γ following stimulation with individual peptides was assayed using an ELISpot assay according to manufacturer's recommendations (Mabtech, Cincinnati, OH). After the *in vitro* expansion step, cells were harvested, washed, and plated in ELISpot plates that were pre-coated with anti-human IL-2 or IFN-γ antibodies. Cells were restimulated with 5 μg/mL peptides and incubated for 24 h at 37°C. Negative controls were treated with media only, and positive controls were treated with either CEFT or phytohemagglutinin (PHA) (Millipore Sigma). Secretions of IL-2 and IFN-γ following the stimulation with peptides were detected using a secondary biotinylated anti-IL-2 or anti-IFN-γ antibody (Mabtech) followed by streptavidin, alkaline phosphatase conjugate (SA-ALP) (Mabtech), nitro blue tetrazolium, and 5-bromo-4-chloro-3′-indolyl phosphate (BCIP/NBT) substrate (KPL, Thermo Fisher Scientific). Computer software (Immunospot 7.0; Cellular Technology, Cleveland, OH) was used to enumerate spots forming cells (SFCs). The assay was performed in triplicate and repeated at least once for each donor.

Flow cytometry

After the *in vitro* expansion step, cells were harvested, washed, and restimulated with 5 μg/mL individual peptides for 24 h at 37°C. Cytokine secretion in cell cultures was blocked by the addition of GolgiPlug/GolgiStop (BD Biosciences, San Jose, CA) for 5 h prior to cell harvesting and staining. Afterward, cells were washed and stained for surface markers CD3 (clone UCHT1), CD4 (clone SK3), CD8 (clone RPA-T8), CD45RA (clone HI100), CD56 (clone HCD56), CCR7 (clone G043H7), and TCRγδ (clone 11F2). Cells were then fixed and permeabilized with Cytofix/Cytoperm solution (BD Biosciences) followed by intracellular staining for cytokines using antibodies against IL-2 (clone MQ1-17H12), IL-4 (clone MP4-25D2), IFN-γ (clone B27), and TNF-α (clone MAb11). Acquisition was performed using a Cytek Aurora (Cytek Biosciences, Fremont, CA), and analysis was performed using Flowjo (Treestar, Ashland, OR) software.

Statistical analysis

Statistical analyses were performed using GraphPad Prism, v.7.0 (GraphPad Software, San Diego, CA). Results are expressed as mean ± SD. Differences between groups were examined for statistical significance using ANOVA with Tukey's multiple comparisons test.

Data and materials availability

All data are available in the main text or the supplemental information.

SUPPLEMENTAL INFORMATION

Supplemental information can be found online at https://doi.org/10.1016/j.omtm.2022.01.005.

ACKNOWLEDGMENTS

This work was supported by the Intramural Research Program of the Center for Biologics Evaluation and Research (CBER), US Food and Drug Administration. This project was also supported in part by S.J.B.'s appointment to the Research Participation Program at CBER administered by the Oak Ridge Institute for Science and Education through the US Department of Energy and US Food and Drug Administration. We thank Suzanne Epstein for critical reading of the manuscript.

AUTHOR CONTRIBUTIONS

Conceptualization, S.J.B. and R.M.; methodology, S.J.B., S.J., W.W.W., A.M.S., S.W., and A.B.; supervision, S.T., R.-F.S., and R.M.; writing – original draft, S.J.B., S.J., W.W.W., A.M.S., and R.M.; writing – review and editing, S.J.B. and R.M.

DECLARATION OF INTERESTS

The authors declare no competing interests.

REFERENCES

1. Goswami, R., Subramanian, G., Silayeva, L., Newkirk, I., Doctor, D., Chawla, K., Chattopadhyay, S., Chandra, D., Chilukuri, N., and Betapudi, V. (2019). Gene therapy leaves a vicious cycle. Front. Oncol. *9*, 297. https://doi.org/10.3389/fonc.2019.00297.

2. Lapteva, L., Purohit-Sheth, T., Serabian, M., and Puri, R.K. (2020). Clinical development of gene therapies: the first three decades and counting. Mol. Ther. Methods Clin. Dev. *19*, 387–397. https://doi.org/10.1016/j.omtm.2020.10.004.

3. Food and Drug Administration (2017). FDA clinical review. Voretigene neparvovec-rzyl (luxturna). https://www.fda.gov/vaccines-blood-biologics/cellular-gene-therapy-products/luxturna.

4. Food and Drug Administration (2019). FDA clinical review. Onasemnogene abeparvovec-xioi (Zolgensma). https://www.fda.gov/vaccines-blood-biologics/zolgensma.

5. Ronzitti, G., Gross, D.A., and Mingozzi, F. (2020). Human immune responses to adeno-associated virus (AAV) vectors. Front. Immunol. *11*, 670. https://doi.org/10.3389/fimmu.2020.00670.

6. Shirley, J.L., de Jong, Y.P., Terhorst, C., and Herzog, R.W. (2020). Immune responses to viral gene therapy vectors. Mol. Ther. *28*, 709–722. https://doi.org/10.1016/j.ymthe.2020.01.001.

7. Mingozzi, F., Maus, M.V., Hui, D.J., Sabatino, D.E., Murphy, S.L., Rasko, J.E., Ragni, M.V., Manno, C.S., Sommer, J., Jiang, H., et al. (2007). CD8(+) T-cell responses to adeno-associated virus capsid in humans. Nat. Med. *13*, 419–422. https://doi.org/10.1038/nm1549.

8. Halbert, C.L., Miller, A.D., McNamara, S., Emerson, J., Gibson, R.L., Ramsey, B., and Aitken, M.L. (2006). Prevalence of neutralizing antibodies against adeno-associated virus (AAV) types 2, 5, and 6 in cystic fibrosis and normal populations: implications for gene therapy using AAV vectors. Hum. Gene Ther. *17*, 440–447. https://doi.org/10.1089/hum.2006.17.440.

9. Calcedo, R., Vandenberghe, L.H., Gao, G., Lin, J., and Wilson, J.M. (2009). Worldwide epidemiology of neutralizing antibodies to adeno-associated viruses. J. Infect. Dis. *199*, 381–390. https://doi.org/10.1086/595830.

10. Boutin, S., Monteilhet, V., Veron, P., Leborgne, C., Benveniste, O., Montus, M.F., and Masurier, C. (2010). Prevalence of serum IgG and neutralizing factors against adeno-associated virus (AAV) types 1, 2, 5, 6, 8, and 9 in the healthy population: implications for gene therapy using AAV vectors. Hum. Gene Ther. *21*, 704–712. https://doi.org/10.1089/hum.2009.182.

11. Manno, C.S., Pierce, G.F., Arruda, V.R., Glader, B., Ragni, M., Rasko, J.J., Ozelo, M.C., Hoots, K., Blatt, P., Konkle, B., et al. (2006). Successful transduction of liver in hemophilia by AAV-Factor IX and limitations imposed by the host immune response. Nat. Med. *12*, 342–347. https://doi.org/10.1038/nm1358.

12. Pien, G.C., Basner-Tschakarjan, E., Hui, D.J., Mentlik, A.N., Finn, J.D., Hasbrouck, N.C., Zhou, S., Murphy, S.L., Maus, M.V., Mingozzi, F., et al. (2009). Capsid antigen presentation flags human hepatocytes for destruction after transduction by adeno-associated viral vectors. J. Clin. Invest. *119*, 1688–1695. https://doi.org/10.1172/jci36891.

13. Konkle, B.A., Walsh, C.E., Escobar, M.A., Josephson, N.C., Young, G., von Drygalski, A., McPhee, S.W.J., Samulski, R.J., Bilic, I., de la Rosa, M., et al. (2021). BAX 335 hemophilia B gene therapy clinical trial results: potential impact of CpG sequences on gene expression. Blood *137*, 763–774. https://doi.org/10.1182/blood.2019004625.

14. Rudolph, M.G., Stanfield, R.L., and Wilson, I.A. (2006). How TCRs bind MHCs, peptides, and coreceptors. Annu. Rev. Immunol. *24*, 419–466. https://doi.org/10.1146/annurev.immunol.23.021704.115658.

15. Hermeling, S., Crommelin, D.J., Schellekens, H., and Jiskoot, W. (2004). Structure-immunogenicity relationships of therapeutic proteins. Pharm. Res. *21*, 897–903. https://doi.org/10.1023/b:pham.0000029275.41323.a6.

16. Petersen, J., Purcell, A.W., and Rossjohn, J. (2009). Post-translationally modified T cell epitopes: immune recognition and immunotherapy. J. Mol. Med. (Berl) *87*, 1045–1051. https://doi.org/10.1007/s00109-009-0526-4.

17. Yang, H., and Zubarev, R.A. (2010). Mass spectrometric analysis of asparagine deamidation and aspartate isomerization in polypeptides. Electrophoresis *31*, 1764–1772. https://doi.org/10.1002/elps.201000027.

18. Chen, W., Ede, N.J., Jackson, D.C., McCluskey, J., and Purcell, A.W. (1996). CTL recognition of an altered peptide associated with asparagine bond rearrangement. Implications for immunity and vaccine design. J. Immunol. *157*, 1000–1005.

19. Cirrito, T.P., Pu, Z., Deck, M.B., and Unanue, E.R. (2001). Deamidation of asparagine in a major histocompatibility complex-bound peptide affects T cell recognition but does not explain type B reactivity. J. Exp. Med. *194*, 1165–1170. https://doi.org/10.1084/jem.194.8.1165.

20. Verma, A., Ngundi, M.M., and Burns, D.L. (2016). Mechanistic analysis of the effect of deamidation on the immunogenicity of anthrax protective antigen. Clin. Vaccin. Immunol. *23*, 396–402. https://doi.org/10.1128/CVI.00701-15.

21. McAdam, S.N., Fleckenstein, B., Rasmussen, I.B., Schmid, D.G., Sandlie, I., Bogen, B., Viner, N.J., and Sollid, L.M. (2001). T cell recognition of the dominant I-A(k)-restricted hen egg lysozyme epitope: critical role for asparagine deamidation. J. Exp. Med. *193*, 1239–1246. https://doi.org/10.1084/jem.193.11.1239.

22. Moss, C.X., Matthews, S.P., Lamont, D.J., and Watts, C. (2005). Asparagine deamidation perturbs antigen presentation on class II major histocompatibility complex molecules. J. Biol. Chem. *280*, 18498–18503. https://doi.org/10.1074/jbc.M501241200.

23. Mamula, M.J., Gee, R.J., Elliott, J.I., Sette, A., Southwood, S., Jones, P.J., and Blier, P.R. (1999). Isoaspartyl post-translational modification triggers autoimmune responses to self-proteins. J. Biol. Chem. *274*, 22321–22327. https://doi.org/10.1074/jbc.274.32.22321.

24. Giles, A.R., Sims, J.J., Turner, K.B., Govindasamy, L., Alvira, M.R., Lock, M., and Wilson, J.M. (2018). Deamidation of amino acids on the surface of adeno-associated virus capsids leads to charge heterogeneity and altered vector function. Mol. Ther. *26*, 2848–2862. https://doi.org/10.1016/j.ymthe.2018.09.013.

25. Rumachik, N.G., Malaker, S.A., Poweleit, N., Maynard, L.H., Adams, C.M., Leib, R.D., Cirolia, G., Thomas, D., Stamnes, S., Holt, K., et al. (2020). Methods matter: standard production platforms for recombinant AAV produce chemically and functionally distinct vectors. Mol. Ther. Methods Clin. Dev. *18*, 98–118. https://doi.org/10.1016/j.omtm.2020.05.018.

26. Madsen, D., Cantwell, E.R., O'Brien, T., Johnson, P.A., and Mahon, B.P. (2009). Adeno-associated virus serotype 2 induces cell-mediated immune responses directed against multiple epitopes of the capsid protein VP1. J. Gen. Virol. *90*, 2622–2633. https://doi.org/10.1099/vir.0.014175-0.

27. Hui, D.J., Edmonson, S.C., Podsakoff, G.M., Pien, G.C., Ivanciu, L., Camire, R.M., Ertl, H., Mingozzi, F., High, K.A., and Basner-Tschakarjan, E. (2015). AAV capsid CD8+ T-cell epitopes are highly conserved across AAV serotypes. Mol. Ther. Methods Clin. Dev. *2*, 15029. https://doi.org/10.1038/mtm.2015.29.

28. Greenbaum, J., Sidney, J., Chung, J., Brander, C., Peters, B., and Sette, A. (2011). Functional classification of class II human leukocyte antigen (HLA) molecules reveals seven different supertypes and a surprising degree of repertoire sharing across supertypes. Immunogenetics *63*, 325–335. https://doi.org/10.1007/s00251-011-0513-0.

29. Weiskopf, D., Angelo, M.A., de Azeredo, E.L., Sidney, J., Greenbaum, J.A., Fernando, A.N., Broadwater, A., Kolla, R.V., De Silva, A.D., de Silva, A.M., et al. (2013). Comprehensive analysis of dengue virus-specific responses supports an HLA-linked protective role for CD8+ T cells. Proc. Natl. Acad. Sci. U S A *110*, E2046–E2053. https://doi.org/10.1073/pnas.1305227110.

30. Becerra, S.P., Koczot, F., Fabisch, P., and Rose, J.A. (1988). Synthesis of adeno-associated virus structural proteins requires both alternative mRNA splicing and alternative initiations from a single transcript. J. Virol. *62*, 2745–2754. https://doi.org/10.1128/jvi.62.8.2745-2754.1988.

31. Sallusto, F., Geginat, J., and Lanzavecchia, A. (2004). Central memory and effector memory T cell subsets: function, generation, and maintenance. Annu. Rev. Immunol. *22*, 745–763. https://doi.org/10.1146/annurev.immunol.22.012703.104702.

32. Takeuchi, A., and Saito, T. (2017). CD4 CTL, a cytotoxic subset of CD4(+) T cells, their differentiation and function. Front. Immunol. *8*, 194. https://doi.org/10.3389/fimmu.2017.00194.

33. Li, H., Lasaro, M.O., Jia, B., Lin, S.W., Haut, L.H., High, K.A., and Ertl, H.C. (2011). Capsid-specific T-cell responses to natural infections with adeno-associated viruses in humans differ from those of nonhuman primates. Mol. Ther. *19*, 2021–2030. https://doi.org/10.1038/mt.2011.81.

34. Veron, P., Leborgne, C., Monteilhet, V., Boutin, S., Martin, S., Moullier, P., and Masurier, C. (2012). Humoral and cellular capsid-specific immune responses to adeno-associated virus type 1 in randomized healthy donors. J. Immunol. *188*, 6418–6424. https://doi.org/10.4049/jimmunol.1200620.

35. Jurtz, V., Paul, S., Andreatta, M., Marcatili, P., Peters, B., and Nielsen, M. (2017). NetMHCpan-4.0: improved peptide-MHC class I interaction predictions integrating eluted ligand and peptide binding affinity data. J. Immunol. *199*, 3360–3368. https://doi.org/10.4049/jimmunol.1700893.

36. Saini, S.K., Hersby, D.S., Tamhane, T., Povlsen, H.R., Amaya Hernandez, S.P., Nielsen, M., et al. (2021). SARS-CoV-2 genome-wide T cell epitope mapping reveals immunodominance and substantial CD8(+) T cell activation in COVID-19 patients. Sci. Immunol. *6*, 1–15. https://doi.org/10.1126/sciimmunol.abf7550.

37. Peters, B., Nielsen, M., and Sette, A. (2020). T cell epitope predictions. Annu. Rev. Immunol. *38*, 123–145. https://doi.org/10.1146/annurev-immunol-082119-124838.

38. Dhanda, S.K., Karosiene, E., Edwards, L., Grifoni, A., Paul, S., Andreatta, M., Weiskopf, D., Sidney, J., Nielsen, M., Peters, B., and Sette, A. (2018). Predicting HLA CD4 immunogenicity in human populations. Front. Immunol. *9*, 1369. https://doi.org/10.3389/fimmu.2018.01369.

39. Mazor, R., Addissie, S., Jang, Y., Tai, C.H., Rose, J., Hakim, F., and Pastan, I. (2017). Role of HLA-DP in the presentation of epitopes from the truncated bacterial PE38 immunotoxin. AAPS J. *19*, 117–129. https://doi.org/10.1208/s12248-016-9986-y.

40. Arentz-Hansen, H., Korner, R., Molberg, O., Quarsten, H., Vader, W., Kooy, Y.M., Lundin, K.E., Koning, F., Roepstorff, P., Sollid, L.M., and McAdam, S.N. (2000). The intestinal T cell response to alpha-gliadin in adult celiac disease is focused on a single deamidated glutamine targeted by tissue transglutaminase. J. Exp. Med. *191*, 603–612. https://doi.org/10.1084/jem.191.4.603.

41. Azam, A., Mallart, S., Illiano, S., Duclos, O., Prades, C., and Maillere, B. (2021). Introduction of non-natural amino acids into T-cell epitopes to mitigate peptide-specific T-cell responses. Front. Immunol. *12*, 637963. https://doi.org/10.3389/fimmu.2021.637963.

42. Benkirane, N., Friede, M., Guichard, G., Briand, J.P., Van Regenmortel, M.H., and Muller, S. (1993). Antigenicity and immunogenicity of modified synthetic peptides containing D-amino acid residues. Antibodies to a D-enantiomer do recognize the parent L-hexapeptide and reciprocally. J. Biol. Chem. *268*, 26279–26285.

43. Nathwani, A.C., Tuddenham, E.G., Rangarajan, S., Rosales, C., McIntosh, J., Linch, D.C., Chowdary, P., Riddell, A., Pie, A.J., Harrington, C., et al. (2011). Adenovirus-associated virus vector-mediated gene transfer in hemophilia B. N. Engl. J. Med. *365*, 2357–2365. https://doi.org/10.1056/NEJMoa1108046.

44. Flotte, T.R.E.-i.-C. (2020). Revisiting the "new" inflammatory toxicities of adeno-associated virus vectors. Hum. Gene Ther. *31*, 398–399. https://doi.org/10.1089/hum.2020.29117.trf.

45. Administration, F.A.D. (2020). Guidance: human gene therapy for hemophilia Janurary 2020. https://www.fda.gov/media/113799/download.

46. Vandamme, C., Adjali, O., and Mingozzi, F. (2017). Unraveling the complex story of immune responses to AAV vectors trial after trial. Hum. Gene Ther. *28*, 1061–1074. https://doi.org/10.1089/hum.2017.150.

47. Yang, F., Patton, K., Kasprzyk, T., Long, B., Gupta, S., Zoog, S.J., et al. (2021). Validation of an IFN-gamma ELISpot assay to measure cellular immune responses against viral antigens in non-human primates. Gene Ther. 1–14. https://doi.org/10.1038/s41434-020-00214-w.

48. Xu, X., Huang, Y., Pan, H., Molden, R., Qiu, H., Daly, T.J., et al. (2019). Quantitation and modeling of post-translational modifications in a therapeutic monoclonal antibody from single- and multiple-dose monkey pharmacokinetic studies using mass spectrometry. PLoS One *14*, 1–26. https://doi.org/10.1371/journal.pone.0223899.

49. Wakankar, A.A., and Borchardt, R.T. (2006). Formulation considerations for proteins susceptible to asparagine deamidation and aspartate isomerization. J. Pharm. Sci. *95*, 2321–2336. https://doi.org/10.1002/jps.20740.

50. Grieger, J.C., Choi, V.W., and Samulski, R.J. (2006). Production and characterization of adeno-associated viral vectors. Nat. Protoc. *1*, 1412–1428. https://doi.org/10.1038/nprot.2006.207.

51. Zolotukhin, S., Byrne, B.J., Mason, E., Zolotukhin, I., Potter, M., Chesnut, K., Summerford, C., Samulski, R.J., and Muzyczka, N. (1999). Recombinant adeno-associated virus purification using novel methods improves infectious titer and yield. Gene Ther. *6*, 973–985. https://doi.org/10.1038/sj.gt.3300938.

52. Sanmiguel, J., Gao, G., and Vandenberghe, L.H. (2019). Quantitative and digital droplet-based AAV genome titration. Methods Mol. Biol. *1950*, 51–83. https://doi.org/10.1007/978-1-4939-9139-6_4.

53. Looze, C., Yui, D., Leung, L., Ingham, M., Kaler, M., Yao, X., Wu, W.W., Shen, R.F., Daniels, M.P., and Levine, S.J. (2009). Proteomic profiling of human plasma exosomes identifies PPARgamma as an exosome-associated protein. Biochem. Biophys. Res. Commun. *378*, 433–438. https://doi.org/10.1016/j.bbrc.2008.11.050.

54. Puig, M., Ananthula, S., Venna, R., Kumar Polumuri, S., Mattson, E., Walker, L.M., Cardone, M., Takahashi, M., Su, S., Boyd, L.F., et al. (2020). Alterations in the HLA-B*57:01 immunopeptidome by flucloxacillin and immunogenicity of drug-haptenated peptides. Front. Immunol. *11*, 629399. https://doi.org/10.3389/fimmu.2020.629399.

55. Reynisson, B., Alvarez, B., Paul, S., Peters, B., and Nielsen, M. (2020). NetMHCpan-4.1 and Netmhcpan-4.0: improved predictions of MHC antigen presentation by concurrent motif deconvolution and integration of MS MHC eluted ligand data. Nucleic Acids Res. *48*, W449–W454. https://doi.org/10.1093/nar/gkaa379.

56. Wang, P., Sidney, J., Kim, Y., Sette, A., Lund, O., Nielsen, M., and Peters, B. (2010). Peptide binding predictions for HLA DR, DP and DQ molecules. BMC Bioinformatics *11*, 568. https://doi.org/10.1186/1471-2105-11-568.

57. Gonzalez-Galarza, F.F., McCabe, A., Santos, E., Jones, J., Takeshita, L., Ortega-Rivera, N.D., Cid-Pavon, G.M.D., Ramsbottom, K., Ghattaoraya, G., Alfirevic, A., et al. (2020). Allele frequency net database (AFND) 2020 update: gold-standard data classification, open access genotype data and new query tools. Nucleic Acids Res. *48*, 783–788. https://doi.org/10.1093/nar/gkz1029.